Multidisciplinary Materials Chronicles, 2025, Vol. X, Iss. X, 112-125

DOI: 10.62184/mmc.jmmc1100202531

Research Article

SCIENCE PARK PUBLISHER

Multidisciplinary Materials Chronicles

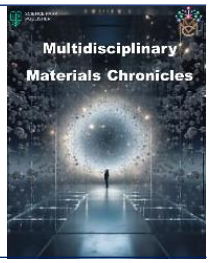

Spatial and temporal assessment of thunderstorm frequency and their impacts on PM2.5 over Iraq

Al-khulaifawi Imad Abdulridha Jasim[1,*], Ioshpa Alexander Ruvimovich[2]

[1] Postgraduate Student, Institute of Earth Sciences, Southern Federal University, Rostov-on-Don, Russian Federation

[2] Department of Oceanology, Institute of Earth Sciences, Southern Federal University, Rostov-on-Don, Russian Federation

Received: 09, 08, 2025; Accepted: 31, 08, 2025; Published: 26, 09, 2025

Abstract

This study analyzes thunderstorm activity based on archival data from daily meteorological observations over 10 years at three meteorological stations in Iraq. The Analysis showed that the highest frequency of thunderstorms occurs in March and April, 45.65%. In Iraq, during the summer, no cases of thunderstorms have been recorded. The highest annual frequency of thunderstorms was recorded at Khanaqin station in 2008 (29 days), while for Baghdad Airport station it was in 2002 (20 days), and for Basra Airport station it was in 2003 (13 days). The particulate matter concentration of 2.5 at the Khanaqin station before, during, and after the storm was (B), while at Basra Airport station was (D). This is a dangerous indicator: the concentration continued to rise without addressing the causes. Burning natural gas and oil is a well-known source of the pollutants that pollute Iraq's air. It appears that the increase in PM2.5 concentrations (D, E, and F ranges) during thunderstorms at stations is due to dry thunderstorms (insufficient relative humidity with no rain) and the downdrafts associated with the storm, causing increased PM2.5 concentrations in the atmosphere for a prolonged period. The frequency of days of thunderstorms and rain (cases) decreases from north to south, while the highest concentration of PM2.5 is from south to north. This suggests that an increase in rainfall leads to a decrease in PM2.5 concentrations. According to the findings from NDDI, 90–95% of Baghdad is situated in areas with low to moderate dust levels for the period 2000-2009, while 90–95% of Baghdad is situated in areas with moderate to high dust levels for the period 2013-2023. which are risk factors for air pollution that affect people's health and well-being.

Keywords: Thunderstorms, Particulate matter PM2.5, Dust storms, Relative humidity, K-index, NDDI

1. Introduction

A thunderstorm is a convective storm that produces lightning and thunder, usually developing within cumulonimbus clouds. When warm, humid surface air is covered by cold, dry air in the atmosphere, the atmosphere becomes conditionally unstable, and a thunderstorm is likely to form. The life cycle of a thunderstorm progresses through three stages. In the developing stage, cumulus clouds grow as rising air currents (updrafts) dominate, with occasional lightning but little or no rain. The storm then enters its mature stage, characterized by simultaneous updrafts and downdrafts as precipitation falls, producing gust fronts and often severe weather such as strong winds, hail, frequent lightning, heavy rain, and occasionally, tornadoes. Finally, in the dissipating stage, downdrafts suppress the updrafts, leading to a rapid decline in storm intensity and widespread precipitation [1]. Storms are of three basic types: single-cell, multicellular, and supercellular storms.

DOI: 10.62184/mmc.jmmc1100202531

Research Article

Thunderstorm formation is driven by three main conditions: (a) atmospheric instability. (b) lifting motion. (c) The amount of moisture in the atmosphere [1]. The National Oceanic and Atmospheric Administration (NOAA) estimated 16 million thunderstorms occur each year. This is equivalent to over 40,000 thunderstorms every day, or roughly 2,000 thunderstorms worldwide at any given time. Every year, there are over 100,000 thunderstorms in the United States alone. About 10% of them are extremely dangerous [2]. Accurate thunderstorm forecasting was improved by satellite data. Geostationary satellite imagery and space-borne lightning observations have enhanced thunderstorm nowcasting (short-term, real-time forecasting), especially in areas where traditional observation networks are sparse. Conventional forecasting techniques were challenging and less dependable, which contributed to a higher number of thunderstorm-related fatalities [3].

Thunderstorm activity is a recognized meteorological mechanism for generating localized dust storms, or haboobs. This phenomenon is a consequence of strong downdrafts and convective outflows that can mobilize surface sediments, a process particularly common in arid environments. Haboobs, which are thunderstorms that produce localized dust storms, are known to occur in Iraq and significantly affect the region's air quality [4, 5].

According to a study, a rise in pollution levels significantly increases the frequency of lightning strikes during atmospheric instability, particularly when those strikes occur from clouds to the ground. This is because pollution enhances the processes within clouds, increasing their strength and activity [6].

Aside from dust, Iraq's air quality has been heavily worsened by human-made sources such as emissions from power plants, widespread use of household and public generators due to electricity shortages, increased transportation activity, fossil fuel combustion for heating, and uncontrolled waste burning, all of which release large amounts of pollutants into the atmosphere [7]. A key concern is fine particulate matter (PM2.5), produced both directly through combustion and secondarily from precursor gases (SO_2, NO_x, NH_3, VOCs). Its small size allows it to remain airborne for prolonged periods, respond strongly to meteorological conditions, and penetrate deep into the respiratory system, posing significant health risks [8, 9]. Beyond dust storms, exposure to air pollution in Iraq contributes to cardiopulmonary diseases, respiratory and eye irritation, and reduced productivity among outdoor and industrial workers, with risks amplified by occupational exposure to mineral, organic, and chemical dusts [10-14]. Additionally, PM10 with an aerodynamic diameter of less than 10 microns is a major concern in Iraq, largely driven by desertification. An ECMWF-based analysis for 2021 showed that PM10 was the dominant pollutant, with the highest levels observed at Rutba, linked to strong vertical transport that enhances convection and daytime storm activity [15]. Another study on PM2.5 (2003–2020) reported higher summer concentrations, peaking in June–July in central and southern Iraq, while the lowest values occurred in November in the north and west [16].

Indices like the K-index, Lifted Index, and Convective Available Potential Energy (CAPE) are crucial for meteorologists to assess regional convective potential. They help pinpoint areas with an unstable atmosphere, which is a key condition for thunderstorm development [17]. While the identification of dust storms in semi-arid regions has been addressed through remote sensing techniques. The Normalized Difference Dust Index (NDDI) and Brightness Temperature Variation (BTV) are two indices that can be used to distinguish dust storm pixels from other features in satellite imagery, allowing the identification of these events in areas that are otherwise difficult to differentiate from desert regions [18].

Numerous studies have investigated thunderstorms. An analysis of the synoptic characteristics, causes, and mechanisms of the Kahlaa tornado event occurred on 14 April 2016 to the north of Kahlaa town in Maysan governorate. The analysis revealed the presence of a low-pressure system, which was an extension of the monsoon low, as well as a supercell thunderstorm and a jet stream aloft. The cold trough and high relative vorticity at the 500 hPa level, along with the humid warm wind blowing from the south and the dry cold wind from the north, contributed to the initiation of the tornado. Three indices were calculated to estimate the instability of the tornado. The values of convective available potential energy (CAPE), K-index, and lifted index were ($\geq$ 2500 J/kg), (35.3 °C), and (-7), respectively [19].

A study on thunderstorm activity in Iraq (1998–2011) identified the area between 35–36°N and 45–46°E as the area most frequently affected by thunderstorms accompanied by lightning. April was found to be the peak month, associated with the Mediterranean low, while the occurrence of the Sudanese low and Red Sea trough further enhanced thunderstorm and lightning

Multidisciplinary Materials Chronicles, 2025, Vol. X, Iss. X, 112-125
DOI: 10.62184/mmc.jmmc1100202531

Research Article

activity [20].

A separate study, monitoring thunderstorm dynamics in Iraq from 2000 to 2009, confirms the seasonal trend, noting that March and April account for nearly half (47.42%) of all thunderstorm activity. It also highlighted the northern mountainous region as a hotspot, accounting for 22.3% of the total thunderstorms. At a more localized level, studies have examined the types of storm systems affecting the country, with one analysis at Khanaqin Station documenting 67 baroclinic and 63 barotropic cases. In contrast, Basra Airport Station, to the south, recorded fewer storms overall, with 21 baroclinic and 27 barotropic cases. The intensification of severe weather, including thunderstorms and heavy rain, is often observed when the Red Sea trough merges with the Mediterranean low, leading to the formation of deep cumulonimbus clouds [21].

This study investigates mesoscale weather patterns associated with thunderstorms and examines variations in PM2.5 concentrations before, during, and after storm events from 2000 to 2009. It further evaluates air quality variability for March and April across selected Iraqi stations and identifies the most polluted location using meteorological and remote sensing data.

2. Materials and methods

Iraq lies in southwestern Asia, northwest of the Arabian Peninsula, between 29˚5′–37˚22′N and 38˚45′–48˚45′E. The country comprises four main physiographic regions with distinct climates: the alluvial plain and desert plateau, characterized by a hot desert climate, the mountainous range with a Mediterranean climate, and the steppe terrain region with a semi-arid climate [22].

Figure 1 shows the topography of Iraq and the locations of the selected stations—Khanaqin, Baghdad Airport, and Basra Airport—with detailed descriptions provided in Table 1.

2.1. Data sources

2.1.1. Meteorological stations observations

Hourly thunderstorm data (including rain or dry) were obtained in real time from the Iraqi Meteorological Organization & Seismology. As shown in Table 1, the data were collected from weather stations distributed across Iraq, with their quality and continuity assessed before analysis.

2.1.2. Reanalysis data (ERA-Interim)

ERA5 is the fifth generation produced by the ECMWF Integrated Forecast System. It incorporates a forecast model with three fully coupled atmosphere, land surface, and ocean wave components. It provides information on a wide range of parameters at the surface (single level) or upper air [23]. The used data have a spatial resolution of 0.25° × 0.25° for the atmosphere at 00, 06, 12, and 18 UTC, temporal resolution for the interval 2000–2009, and pressure levels of 850,700,500 hPa. The model synopsis is summarized in Table 2.

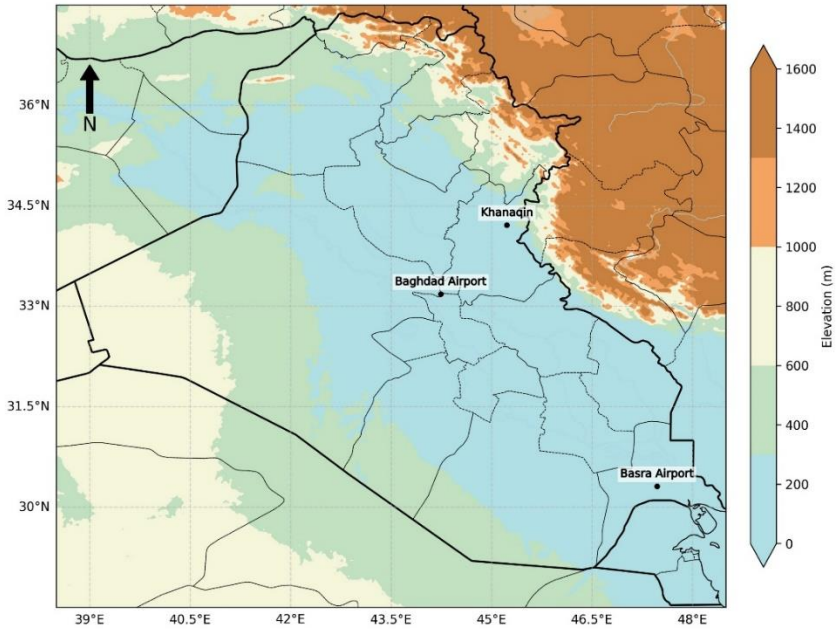

Figure 1. Map of Iraq with the selected stations.

Multidisciplinary Materials Chronicles, 2025, Vol. X, Iss. X, 112-125
DOI: 10.62184/mmc.jmmc1100202531

Research Article

Table 1. Weather Stations Information.

Station	Station number	Longitude	Latitude	Height(m)
Khanaqin	637	45.23° N	34.21° E	202
Baghdad Airport	650	44.24° N	33.18° E	31.7
Basra Airport	690	47.47° N	30.31° E	2.6

Table 2. Overview of the ERA5 driving model.

Characteristics	ERA- (ERA5)
Horizontal coverage	Global
Vertical coverage	1000 hPa to 1 hPa
Output	each 6h for upper-air
Horizontal resolution	Reanalysis: 0.25° × 0.25°
Vertical resolution	37 pressure levels
Data assimilation	yes

2.1.3. Reanalysis data (MERRA-2)

The Modern-Era Retrospective Analysis for Research and Applications, Version 2 (MERRA-2), is a comprehensive atmospheric reanalysis dataset from NASA's Global Modeling and Assimilation Office (GMAO). Released in 2017, MERRA-2 provides a wide range of atmospheric data, including a continuous record of aerosols from 1980 to the present. The dataset features a high spatial resolution of 0.5° x 0.625° and utilizes 72 vertical layers that extend beyond 80 km. This is achieved by combining the Goddard Earth Observing System, version 5 (GEOS-5) model with the Goddard Chemistry Aerosol Radiation and Transport (GOCART) model [24, 25].

This study uses bias-corrected global hourly surface PM2.5 mass concentration data spanning the period from 2000 to 2009. Developed for the NASA Health and Air Quality Applied Sciences Team (HAQAST), this data was generated using a machine learning approach that employs a convolutional neural network (CNN) [26]. The criteria for classifying PM2.5 concentration are detailed in Table 3.

.

Table 3. Classification of PM2.5 concentrations.

PM2.5	Concentration (μg/m^3)
A	(0-12)
B	(12.1-35.4)
C	(35.5-55.4)
D	(55.5-150.4)
E	(15.5-250.4)
F	(250.5-500.4)

Table 4. Overview of the Landsat-8 model.

Characteristics	NASA/ Landsat-8
Spatial resolution	15 m (panchromatic), 30 m (multispectral), 100 m (thermal)
Spectral bands	11 bands, covering coastal, NIR, SWIR, and thermal
Scene size	185 × 180 km

Multidisciplinary Materials Chronicles, 2025, Vol. X, Iss. X, 112-125
DOI: 10.62184/mmc.jmmc1100202531

Research Article

2.1.4. Landsat-8 data

The study utilized Landsat-8 Operational Land Imager (OLI) imagery to analyze dust activity in Baghdad, Iraq, an area known for its arid environment. Surface reflectance data (Collection 2, Tier 1 Level-2) were processed via the Google Earth Engine (GEE) platform. The 30-meter spatial resolution of Landsat-8's visible and near-infrared bands was ideal for analyzing dust in both urban and semi-arid areas. To quantify and visualize the spatial distribution of dust, each pixel in the resulting map was classified based on its Normalized Difference Dust Index (NDDI) range [27]. Table 4 represents the data summary.

2.2. The calculations of some indices

2.2.1. K-index

Temperature (T) and relative humidity (RH) were used to calculate the dew point (Td) and the Dew Point Depression (DD=T-Td), which was then used to calculate the K-index as in equations (1) and (2).

Td = (243.04 * [ln(RH / 100) + ((17.625 * T) / (243.04 + T))]) / (17.625 - [ln(RH / 100) + ((17.625 * T) / (243.04 + T))]) [28]. (1)

K = T (850 mb) + Td (850 mb) – T (500mb) – DD (700 mb) [29]. (2)

A potential thunderstorm can be determined by the value of the K-index as shown in table 5.

Table 5. Atmospheric stability is based on the K-index value [29].

Number	K-Index Value (°C)	Thunderstorm Probability (Types)
1	K below 20	None
2	K between 20 to 25	Isolated thunderstorms
3	K between 26 to 30	Widely scattered thunderstorms
4	K over 31 to 35	Scattered thunderstorms
5	K = 40 or Above 35	Numerous thunderstorms

2.2.2. NDDI calculation

The Normalized Difference Dust Index (NDDI) was employed to detect and assess dust concentration. NDDI is calculated using surface reflectance values from the red and blue bands as in equation (3):

$$NDDI = \frac{(R_{Red} - R_{Blue})}{(R_{Red} + R_{Blue})} \qquad (3)$$

Where: R_{Red} is the surface reflectance from Band 4 (Red: 0.640–0.670 m), R_{Blue} is from Band 2 (Blue: 0.450–0.510 m).

All Landsat-8 scenes were filtered by cloud cover (< 20%) and further refined using pixel-level quality assurance (QA_PIXEL) masks to exclude cloud and shadow contamination. Surface reflectance values were converted using scale factors provided by USGS documentation.

Each image was masked, and NDDI was computed for each scene. All valid NDDI values were then combined to generate a mean annual NDDI maps for (2000-2009) and (2013-2023). To provide a more interpretable analysis of dust severity [30]. The continuous NDDI values were classified into six discrete dust intensity classes as in Table 6.

Table 6. NDDI-based classification of dust severity in the study area [30].

Class	NDDI Range	Description
1	≤ 0.00	No dust / Vegetation
2	0.00 – 0.10	Very low dust
3	0.10 – 0.20	Low dust
4	0.20 – 0.30	Moderate dust
5	0.30 – 0.40	High dust
6	> 0.40	Severe dust / Dust storm

Multidisciplinary Materials Chronicles, 2025, Vol. X, Iss. X, 112-125
DOI: 10.62184/mmc.jmmc1100202531

Research Article

3. Results and discussion

3.1. Analysis of the nature and distribution of thunderstorms with the main observation time

Over the 10-years period, a total of 351 days with thunderstorms were recorded across the three stations. Khanaqin, located in mountainous terrain, experienced the highest frequency (182 days), Baghdad Airport recorded 102 days, and Basra Airport, located near the North of the Arabian Gulf, had the lowest frequency (67 days). The highest annual frequency of thunderstorms was for Khanaqin station in 2008 (29 days), while for Baghdad Airport station it was in 2002 (20 days), and for Basra Airport station it was in 2003 (13 days), Figure 2. On the other hand, thunderstorms are more frequent throughout the country in spring (March-April) [31, 32].

An analysis of the average monthly number of days with thunderstorms over 10 years (from 2000 to 2009) at all stations in Iraq revealed that the maximum frequency of thunderstorm activity occurs in spring, in March and April, accounting for about 45.65% of all thunderstorms. However, April has the highest value for the recurrence of storms (Figure 3) [21].

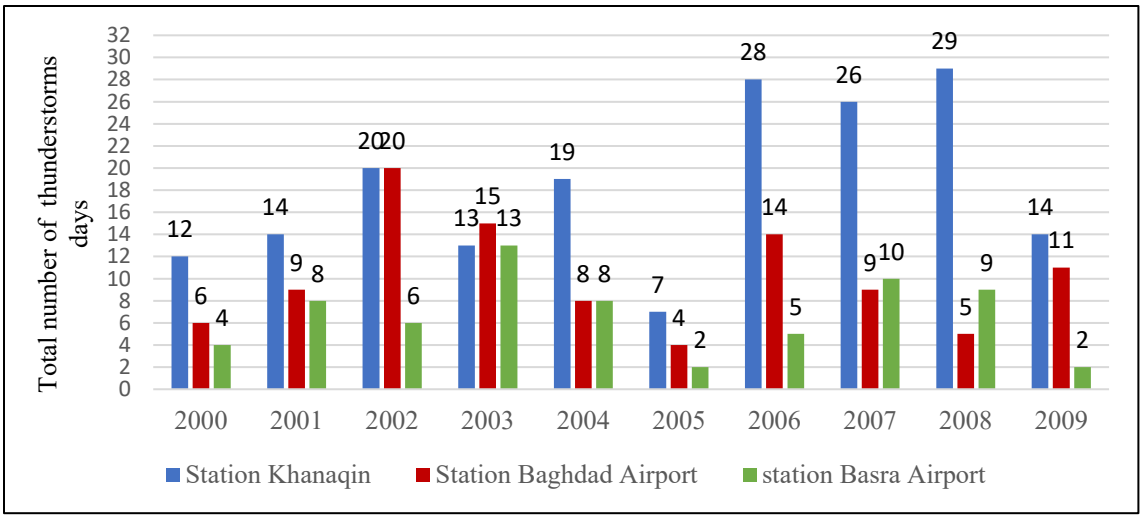

Figure 2. Annual distribution of thunderstorms for 2000-2009.

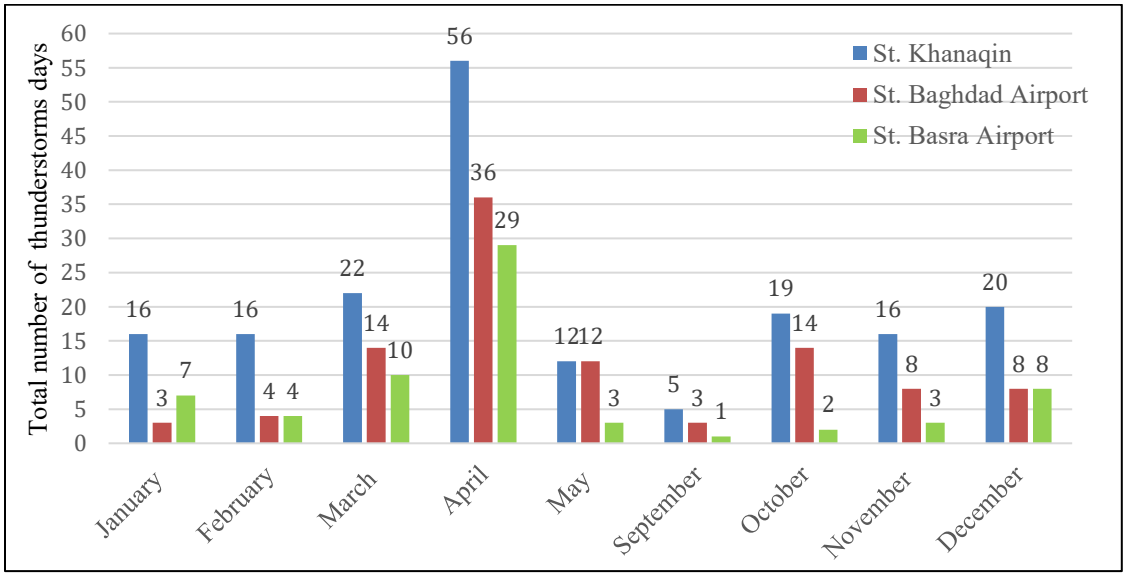

Figure 3. Monthly distribution of thunderstorms for 2000-2009.

Multidisciplinary Materials Chronicles, 2025, Vol. X, Iss. X, 112-125
DOI: 10.62184/mmc.jmmc1100202531

Research Article

Table 7 shows the values of the air stability index, which is classified into five categories. The most frequently occurring value is (K between 26 and 30) at Baghdad Airport and Khanaqin (widely scattered thunderstorms), while the most common value is (K between 31 and 35) at Basra Airport (scattered thunderstorms). Throughout the study, the reason for the increased frequency of thunderstorms at the station is their height above sea level (202 m) due to orographic lifting compared to lowland sites.

By analyzing nine months of data from Khanaqin, Baghdad Airport, and Basra Airport stations, the results indicated that the best time for thunderstorms to recur is 18:00, except for the Baghdad Airport station, which is 06:00 AM. The lowest times for thunderstorms at Khanaqin station are 06:00 AM, while at Baghdad Airport station it is 00:00, and for Basra Airport station it is 12:00 PM

3.2. The impact of thunderstorms on (PM2.5) in Iraq

Results of the impact of thunderstorms on PM2.5 and their frequencies are shown in Figures 4, 5, and 6 and summarized in Table 8. These results are based on PM2.5 concentrations measured before, during, and after thunderstorms at Khanaqin, Baghdad Airport, and Basra Airport stations, as well as on hourly data of thunderstorms (both wet and dry) for March and April, from 2000 to 2009.

The results shown in Figure 4 indicate that the (B) level accounts for 50% the frequency of PM2.5. This is because large areas of agricultural land and the absence of an asphalt plant and an oil refinery in the city. Additionally, a smaller population and fewer cars and generators, compared to the provincial center (Diyala), contribute to this. Therefore, the concentration of PM2.5 is low (indicating clean or moderate air). Not all thunderstorms at Khanaqin station are accompanied by rain (the reason is that there is no enough moisture in the atmosphere), so the concentration does not decrease to a (A) level due to the increase in dust and pollutants caused by the downdrafts and updrafts of thunderstorms.

3.2.1. Khanaqin station

- Before 1h of a thunderstorm: The majority of PM2.5 frequencies fall within the (B) (12.1-35.4 μg/m³) and (C) (35.5-55.4 μg/m³) ranges. A significant number of frequencies also fall into the (D) category (55.5-150.4 μg/m³), with a small frequency of (A) quality air.
- During a thunderstorm: There is a slight decrease in the frequency of PM2.5 in the (B) (predominant frequency) and (C) ranges. The frequency of the (D) category appears to increase, indicating a possible rise in PM2.5 during the storm.
- After 1h of thunderstorm: The frequencies return to a pattern similar to the period before the thunderstorm, suggesting that any changes during the event were temporary. The highest frequencies are again in the (B) and (C) ranges.

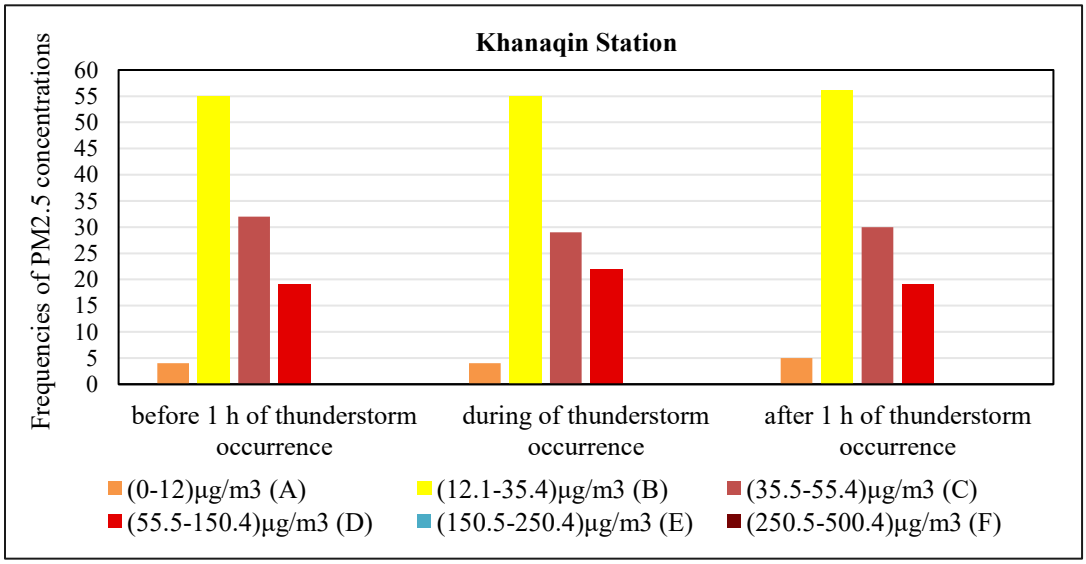

Figure 4. Temporal analysis of air quality status: Mean frequencies of PM2.5 concentration levels (April-May, 2000-2009) for Khanaqin station.

DOI: 10.62184/mmc.jmmc1100202531

Research Article

Table 7. Frequency of air stability index (2000-2009).

Stations	K below 20	K between 20 to 25	K between 26 to 30	K between 31 to 35	K = 40 or Above 35	Total frequency (cases)
Khanaqin	37	61	96	75	8	277
Baghdad Airport	11	30	44	34	7	126
Basra Airport	23	17	25	32	6	103

Figure 5 shows that the concentration of PM2.5 is at three levels: groups (B), (C), and (D), each in different proportions. The reason is the lack of high humidity in the air (according to the Iraqi Meteorological Organization). Another reason is that this is the result of the wind carrying dust from western Iraq (the desert). Additionally, Baghdad has millions of cars and a large population, along with urban development, and the destruction of agricultural land due to drought and lack of rain. Therefore, the concentration has not decreased.

3.2.2. Baghdad Airport station

- Before 1 h of a thunderstorm: Most of PM2.5 frequencies fall within the (B) (12.1-35.4 μg/m³), (C) (35.5-55.4 μg/m³), and (D) (55.5-150.4 μg/m³) ranges. A significant number also falls into the (D) category (55.5-150.4 μg/m³), with a small frequency of (E) air.
- During a thunderstorm: There is a slight decrease in the frequency of PM2.5 in the (C) (prevailing frequency) and (D) ranges. The frequency of the (B) category appears to increase, with a small frequency of (E) (15.5-250.4 μg/m³) and (F) (250.5-500.4 μg/m³) air, indicating a rise in PM2.5 during the storm.
- After 1 h of a thunderstorm, we observe an increase in the frequency of PM2.5 in the (B) frequency, with a decrease in frequencies in the (C) and (D) ranges. This indicates a possible decrease in PM2.5 after the storm.

Figure 6 shows that the concentration of PM2.5 recorded (D) levels approximately 50% of thunderstorm frequency, In recent years, high concentrations of air pollution have been recorded as a result of waste incineration and destruction of green spaces, estimated at 10-15% (unlike in the nineties, there were many green spaces here), and this city is characterized by a large number of oil wells (it is considered the first oil field in Iraq), as well as millions of vehicles, running on fuel. Since 2003, the number of people who have cancer and other diseases has reached an all-time high. According to previous studies, the wind direction accompanying storms is north and northwest prevailing.

3.2.3. Basra Airport station

- Before 1 h of a thunderstorm: Most of PM2.5 frequencies fall within the (D) category (55.5-150.4 μg/m³). A significant number also falls into the (B) (12.1-35.4 μg/m³) and (C) (35.5-55.4 μg/m³) ranges, with a very small frequency in the (F) (250.5-500.4 μg/m³) air.
- During a thunderstorm: There is a slight decrease in the frequency of PM2.5 in the (C) and (E) ranges. The frequency of the (D) (prevailing frequency) and (F) ranges appears to increase, indicating a rise in PM2.5 during the storm.
- After 1 h of a thunderstorm, we observe an increase in the frequency of PM2.5 in the (C) and (E) ranges, with a decrease in frequencies in the (B) category. This indicates a possible or light rise in PM2.5 after the storm.

From table 8, we observe that the frequency of thunderstorms and rainy days (cases) decreases from north to south, while the highest concentration of PM2.5 is from south to north. This indicates that an increase in rainfall leads to a decrease in concentrations of PM2.5. Emissions from brick factories account for 15% of air pollution in Baghdad (Ministry of Environment Report for 2023). The first reason is caused by car exhausts, which reach 40% (the number of cars in Baghdad for 2023 is almost 3 million), and the second is emissions from civilian power generators due to government power outages, which also reached 40%.

Multidisciplinary Materials Chronicles, 2025, Vol. X, Iss. X, 112-125
DOI: 10.62184/mmc.jmmc1100202531

Research Article

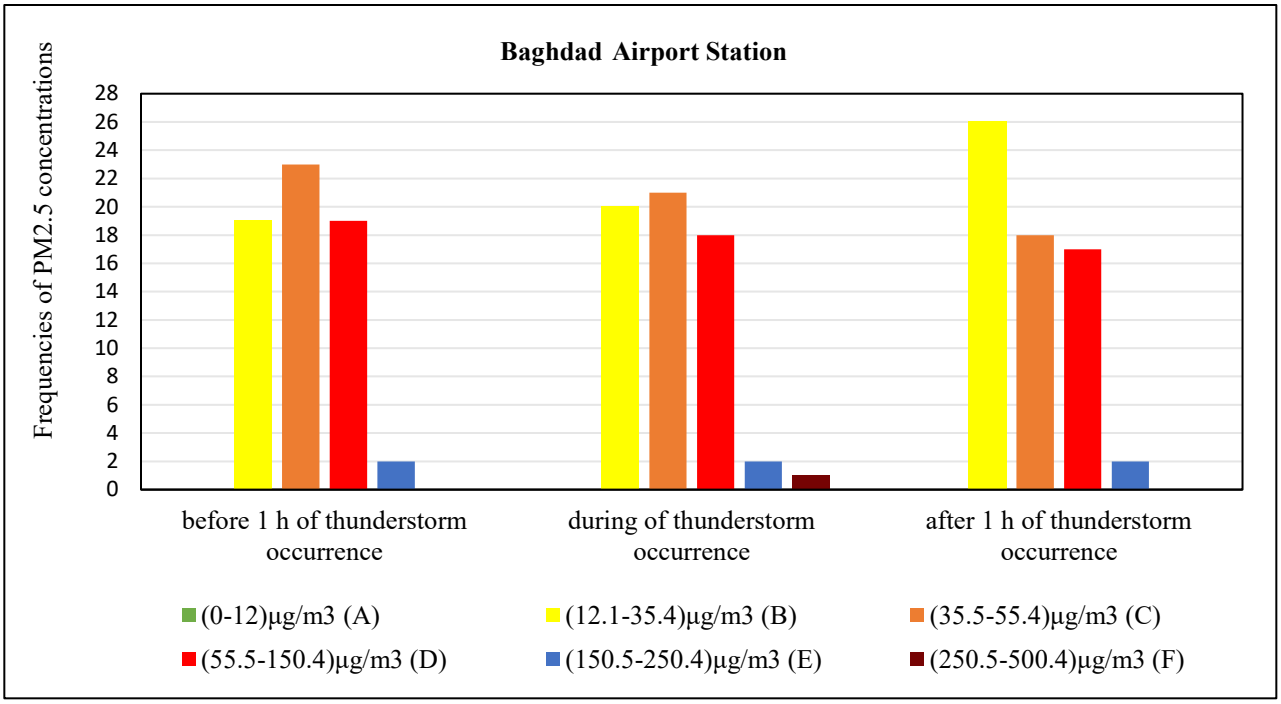

Figure 5. Temporal analysis of air quality status: Mean frequencies of PM2.5 concentration levels (April-May, 2000-2009) at Baghdad Airport station.

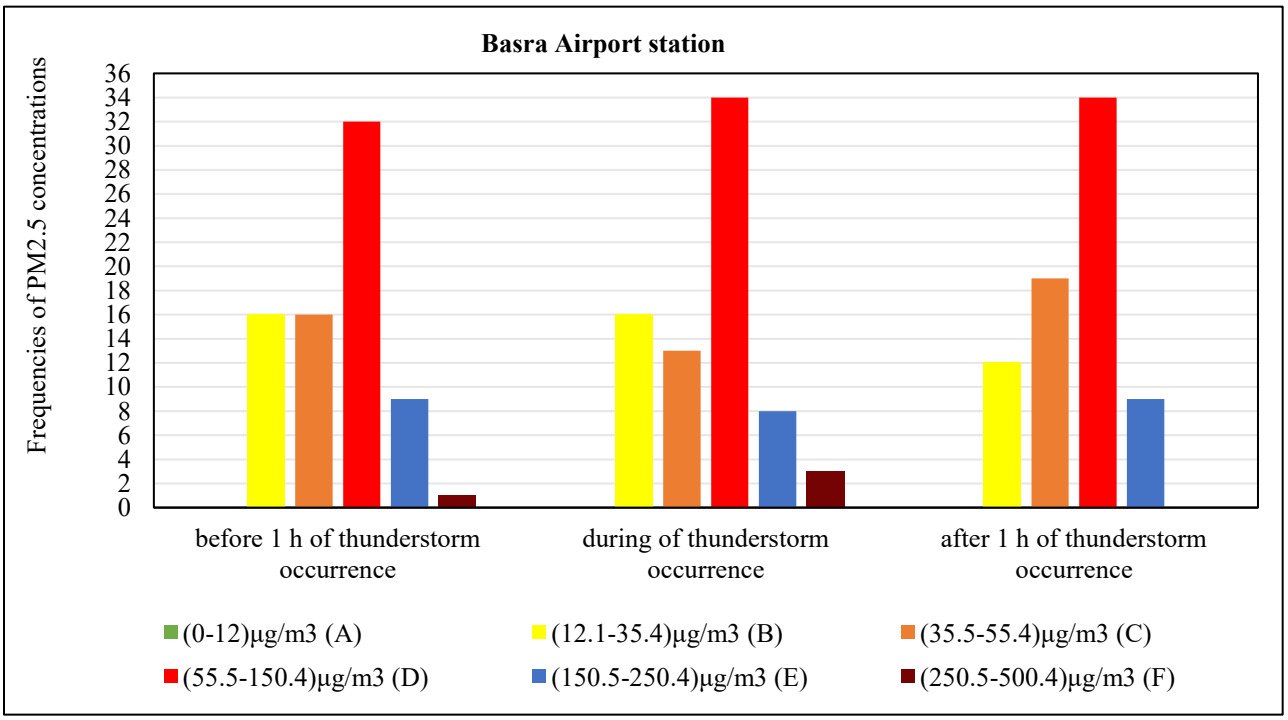

Figure 6. Temporal analysis of air quality status: Mean frequencies of PM2.5 concentration levels (April-May, 2000-2009) for Basra Airport station.

Multidisciplinary Materials Chronicles, 2025, Vol. X, Iss. X, 112-125
DOI: 10.62184/mmc.jmmc1100202531

Research Article

Table 8. Summarizes the results (thunderstorms and PM2.5) for three meteorological stations during the period (2000-2009).

Station	Thunderstorm Days	Total Thunderstorm Events	Events with Rain	Events no Rain	Highest rate PM2.5 before 1 h	Highest rate PM2.5 during 1 h	Highest rate PM2.5 after 1 h	Sources of Pollution
Khanaqin	78 days	110 cases	38 cases	72 cases	(B)	(B)	(B)	Power plants, brick factory, vehicle exhausts.
Baghdad Airport	49 days	63 cases	20 cases	43 cases	(C)	(C)	(B)	Petrochemical Plant, Oil Refinery, Power plant, Brick and Asphalt factory, Food factory, waste incineration, agricultural land removal, burning of crude oil and gas, vehicle exhausts, generators.
Basra Airport	39 days	74 cases	13 cases	61 cases	(D)	(D)	(D)	Petrochemical plant, Oil Refinery, Oil Wells, Power plant, Brick and Asphalt factory, Food factory, Steel and Iron foundry, waste incineration, agricultural land removal, burning of crude oil and gas, vehicle exhausts.

3.3. NDDI map analysis: 2000-2009 versus 2013-2023 for Baghdad

To evaluate the severity of dust at Baghdad station, NDDI was calculated and analyzed based on Table 6 for two periods: 2000-2009 and 2013-2023. The results are presented in Figures 7 and 8. A comparative analysis of NDDI maps for Baghdad reveals a notable increase in the severity of dust events between the two periods:

The map for the first period (Figure 7) shows mostly low to moderate dust levels, represented by yellow shades (NDDI 0.10–0.30). Areas with a high dust concentration (NDDI 0.30–0.40), shown in orange, are present but not widespread. Importantly, the lack of the red category (NDDI > 0.40) indicates that severe dust events were not a characteristic feature of the long-term mean during this decade. The green-shaded regions (NDDI ≤ 0.10) mark areas with minimal dust, particularly along the Tigris River, where water likely helps reduce dust.

In contrast, the map for the second period (Figure 8) shows a significant escalation in dust intensity. Although the main yellow and orange patterns persist, the appearance of red pixels indicates that dust levels have often exceeded the 0.40 threshold, signaling severe dust events or dust storms. These intense dust conditions are particularly evident in the northern and southern parts of the mapped area. This indicates a significant decline in air quality related to dust over the past decade.

Multidisciplinary Materials Chronicles, 2025, Vol. X, Iss. X, 112-125

DOI: 10.62184/mmc.jmmc1100202531

Research Article

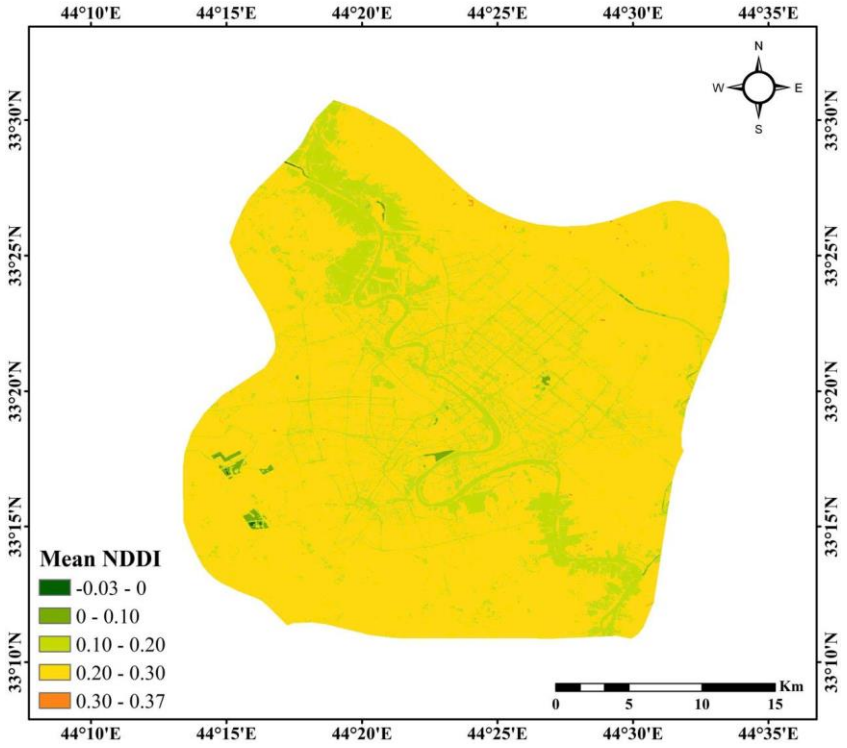

Figure 7. Annual average NDDI map, classified by five levels of dust intensity in Baghdad (2000-2009).

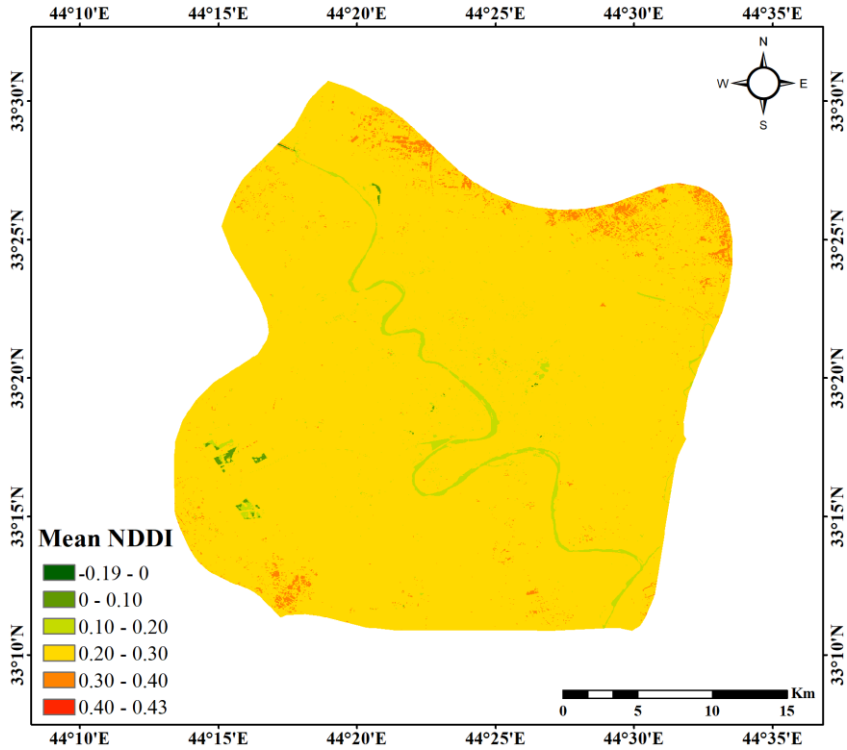

Figure 8. Annual average NDDI map, classified by six levels of dust intensity in Baghdad (2013-2023).

DOI: 10.62184/mmc.jmmc1100202531

Research Article

Thus, there is a rise in both the frequency and intensity of dust events in Baghdad. The transition from a landscape mostly affected by low and moderate dust to one that experiencing severe dust events indicates a worrying trend, probably driven by environmental factors such as desertification and land-use changes.

4. Conclusion

Based on the analysis of the frequency of thunderstorms in the study area, it can be concluded that:

1- A high level of thunderstorm activity was observed in the northern and northeastern parts of Iraq (at the Khanaqin station).

2- The highest frequency of thunderstorms in Iraq occurs in the annual cycle from March to April. At Khanaqin station, Baghdad Airport, and Basra, the highest number of days was in April (56, 36, and 29 days), respectively.

3- The highest annual frequency of thunderstorms was recorded at Khanaqin station in 2008 (29 days), at Baghdad Airport Station in 2002 (20 days), and at Basra Airport station in 2003 (13 days).

4- The highest concentration of particulate matter is 2.5 (B). It was at Khanaqin Station before, during, and after the thunderstorm, which means that the air pollution concentration is within the clean level. However, Basra Airport Station recorded the worst concentration of 2.5 (D) particulates before, during, and after the thunderstorm. The concentration of air pollution is within the non-permissible level. Meanwhile, the Baghdad Airport station recorded a particle concentration of 2.5 (C) before and during the storm, and after the storm, the concentration of 2.5 was (B).

5- The NDDI for the city of Baghdad from 2000 to 2009 is not a reliable indicator, while the period from 2013 to 2023 is considered a reliable indicator.

Conflict of Interest Statement

The authors declare that they have no conflicts of interest to report.

Funding Statement

This research did not receive any specific grant from funding agencies in the public, commercial, or not-for-profit sectors.

Author information

Corresponding author: Al-khulaifawi Imad Abdulridha Jasim*

E-mail: imadjasim900@gmail.com

ORCID iD: 0009-0008-1610-9795

References

[1] R. Stull, Practical Meteorology: An Algebra-based survey of atmospheric science. Univ. of British Columbia, Vancouver, BC, Canada, 2017, ISBN 9780888652836.

[2] J. Dudhia, Back to basics: thunderstorms: part I. Weather, 51 (1996) 371-376. https://doi.org/10.1002/j.1477-8696.1996.tb06162.x.

[3] S. Chaudhuri, A. Middey, Nowcasting lightning flash rate and peak wind gusts associated with severe thunderstorms using remotely sensed TRMM-LIS data, IJRS. 34 (2013) 1576-1590. http://doi.org/10.1080/01431161.2012.723834.

[4] Y. Shao, Physics and modelling of wind erosion, Atmospheric and Oceanographic Sciences Library, Springer, Netherlands, 2008. https://doi.org/10.1007/978-1-4020-8895-7.

[5] M.F. Al-Zuhairi, J.H. Kadhum, Spatiotemporal distribution of the Aura-OMI aerosol index and dust storm case studies over Iraq, Arab. J. Geosci. 14 (2021) 909. http://doi.org/10.1007/s12517-021-07276-z.

[6] J. Sae-Jung, M. Bentley, T. Gerken, The impact of Urban particulate matter on lightning frequency in thunderstorms: a case study of the Bangkok Metropolitan region, Earth Syst. Environ. (2024) Article 138. https://doi.org/10.1007/s41748-024-00474-1.

[7] M. Al-Kasser, Evaluation the level of some toxic pollutants in atmospheric total suspended particles in Al-Diwaniya City – Iraq, Ph.D. Thesis, Faculty of Science, Al-Qadisiyah University, 2018.

[8] W. M. Hodan, W. R. Barnard, Evaluating the contribution of PM2.5 precursor gases and re-entrained road emissions to mobile source PM2.5 particulate matter emissions, MACTEC Federal Programs, Research Triangle Park, North Carolina, USA, 2004.

[9] X. J. Zhang, J. Zhong, Y. Wang, Y. Liu, The interdecadal worsening of weather conditions affecting aerosol pollution in the Beijing area in relation to climate warming, Atmos. Chem.

DOI: 10.62184/mmc.jmmc1100202531

Research Article

Phys. 18(2018) 5991-5999. https://doi.org/10.5194/acp-18-5991-2018.

[10] A.S.V. Shah, J.P. Langrish, H. Nair, D. A. McAllister, A. L. Hunter, K. Donaldson, D. E. Newby, N.L. Mills, Global association of air pollution and heart failure: A systematic review and meta-analysis, Lancet. 382 (2013) 1039–1048. https://doi.org/10.1016/S0140-6736(13)60898-3.

[11] S.J. Jung, J.S. Mehta, L. Tong, Effects of environmental pollution on the ocular surface, Ocul. Surf. 16 (2018) 198–205. https://doi.org/10.1016/j.jtos.2018.03.001.

[12] R. Burnett, H. Chen, M. Szyszkowicz, N. Fann, B. Hubbell, C.A. Pope, J.S. Apte, M. Brauer, A. Cohen, S. Weichenthal, et al. Global estimates of mortality associated with long-term exposure to outdoor fine particulate matter, Proc. Natl. Acad. Sci. USA. 115 (2018) 9592–9597. https://doi.org/10.1073/pnas.1803222115.

[13] S. Arslan, A. Aybek, Particulate matter exposure in agriculture, Air Pollut. A Compr. Perspect. 3 (2012). https://doi.org/10.5772/50084.

[14] A.A. Almetwally, M. Bin-Jumah, A. Allam, Ambient air pollution and its influence on human health and welfare: An overview, Environ. Sci. Pollut. Res. 27 (2020) 24815–24830. https://doi.org/10.1007/s11356-020-09042-2.

[15] Z. Abbood, M. Khalaf, O. Al-Taai, Temporal and spatial analysis of particulate matter concentrations in Iraq. IOP Conference Series, Earth Environ. Sci. 1215 (2023) 012018. https://doi.org/10.1088/1755-1315/1215/1/012018.

[16] M.W. Sadar, H.M. Al-Jiboori, K. Y. Al-Timimi, Spatial analysis of PM2.5 concentration over Iraq during 2003-2020, J. Earth Space Phys. 48 (2023) 173-182. http://doi.org/10.22059/jesphys.2022.344671.1007441.

[17] B.Y. Humood, L.M. Abbas, Studying recorded lightning over Iraq for period 1998-2011, Al-Mustansiriyah J. Sci. 28 (2017) 1-6. http://doi.org/10.23851/mjs.v28i3.50.

[18] N.k. ghazal, Monitoring dust storm using Normalized difference dust index (NDDI) and brightness temperature variation in Simi arid areas over Iraq, Iraqi J. Phys. 18 (2020) 68-75. https://doi.org/10.30723/ijp.v18i45.517.

[19] T.O. Roomi, F.S. Basheer, The Synoptic characteristics, causes, and mechanisms of kahlaa tornado in Iraq on 14th April 2016, Baghdad Sci. J. 18 (2021) 1038-1047. https://doi.org/10.21123/bsj.2021.18.2(Suppl.).1038.

[20] L. M. Abbas, Evaluate thunderstorms and lightning distribution and their relationship with some meteorological parameters in Iraq, M.Sc. Thesis, College of Science, Al-Mustansiriyah University, 2017.

[21] I.A. Al-Khulaifawi, A.R. Ioshpa, Monitoring of monthly dynamics of thunderstorm activity in Iraq. Izvestiya of Saratov University. Earth Sci. 24 (2024) 4-10. https://doi.org/10.18500/1819-7663-2024-24-1-4-10.

[22] N. Al-Ansari, Topography and climate of Iraq, J. Earth Sci. Geotech. Eng. 11 (2021) 1-13. http://doi.org/10.47260/jesge/1121.

[23] H. Hersbach, B. Bell, P. Berrisford, G. Biavati, A. Horányi, J. Muñoz Sabater, J. Nicolas, C. Peubey, R. Radu, I. Rozum, D. Schepers, A. Simmons, C. Soci, D. Dee, J-N. Thépaut, ERA5 hourly data on pressure levels from 1940 to present, Copernicus Climate Change Service (C3S) Climate Data Store (CDS) 2023. https://doi.org/10.24381/cds.bd0915c6.

[24] V. Buchard, C.A. Randles, A.M. da Silva, A. Darmenov, P.R. Colarco, R. Govindaraju, R. Ferrare, J. Hair, A.J. Beyersdorf, L.D. Ziemba, H. Yu, The MERRA-2 aerosol reanalysis, 1980 onward. Part II: evaluation and case studies, J. Clim, 30 (2017) 6851–6872. https://doi.org/10.1175/JCLI-D-16-0613.1.

[25] P. Colarco, A. da Silva, M. Chin, T. Diehl, Online simulations of global aerosol distributions in the NASA GEOS-4 model and comparisons to satellite and ground-based aerosol optical depth, J. Geophys. Res. 115 (2010) D14207. https://doi.org/10.1029/2009JD012820.

[26] P. Gupta, A. Sayeed, MERRA2_CNN_HAQAST bias corrected global hourly surface total PM2.5 mass concentration, V1, Greenbelt, MD, USA, Goddard Earth Sciences Data and Information Services Center (GES DISC), (2024). https://doi.org/10.5067/OCKK5HCFW5N3 (Accessed July 10, 2025).

[27] United States Geological Survey (USGS), Landsat Data Resources, Retrieved from: https://landsat.gsfc.nasa.gov/data/data-resources/#:~:text=USGS%20Resources,Cloud%2C%20and%20the%20LandsatLook%20Viewer. (Accessed July 15, 2025).

[28] A. L. Buck, New equations for computing vapor pressure and enhancement factor, J. Appl. Meteorol. 20 (1981) 1527-1532.

DOI: 10.62184/mmc.jmmc1100202531

Research Article

https://doi.org/10.1175/15200450(1981)020%3C1527:nefcvp%3E2.0.co;2.

[29] J. J. George, Weather Forecasting for Aeronautics, Academic Press, Waltham, MA, 1960. https://doi.org/10.1016/b978-1-4832-3320-8.50004-2.

[30] D. Xu, J.J. Qu, S. Niu, X. Hao, Sand and dust storm detection over desert regions in China with MODIS measurements, Int. J. Remote Sens. 32 (2011) 9365–9373. https://doi.org/10.1080/01431161.2011.556679.

[31] A. R. Ioshpa, I. A. D. Al-Khulaifawi, Analysis of thunderstorm activity in Iraq, Bull. High. Educ. Inst. North Caucasus Reg., Nat. Sci. 218 (2023) 75-80. https://doi.org/10.18522/1026-2237-2023-2-75-80.

[32] I.A.D. Al-Khulaifawi, A.R. Ioshpa, Analysis of thunderstorm activity in Iraq and Turkey. news of the Ural State Mining University. Series: Discussion Club, 4 (2023) 164-169. https://doi.org/10.18522/1026-2237-2023-2-75-80.